Available online at www.sciencedirect.com

SCIENCE DIRECT

Developmental Biology 272 (2004) 161–175

DEVELOPMENTAL BIOLOGY

www.elsevier.com/locate/ydbio

The role of *Pax2* in mouse inner ear development

Quianna Burton, Laura K. Cole, Michael Mulheisen, Weise Chang, and Doris K. Wu*

National Institute on Deafness and Other Communication Disorders, Bethesda, MD 20892, USA

Received for publication 29 January 2004, revised 1 April 2004, accepted 13 April 2004

Abstract

The paired box transcription factor, Pax2, is important for cochlear development in the mouse inner ear. Two mutant alleles of *Pax2*, a knockout and a frameshift mutation (*Pax2*^{1Neu}), show either agenesis or severe malformation of the cochlea, respectively. In humans, mutations in the *PAX2* gene cause renal coloboma syndrome that is characterized by kidney abnormalities, optic nerve colobomas and mild sensorineural deafness. To better understand the role of Pax2 in inner ear development, we examined the inner ear phenotype in the *Pax2* knockout mice using paint-fill and gene expression analyses. We show that *Pax2* −/− ears often lack a distinct saccule, and the endolymphatic duct and common crus are invariably fused. However, a rudimentary cochlea is always present in all *Pax2* knockout inner ears. Cochlear outgrowth in the mutants is arrested at an early stage due to apoptosis of cells that normally express *Pax2* in the cochlear anlage. Lack of *Pax2* affects tissue specification within the cochlear duct, particularly regions between the sensory tissue and the stria vascularis. Because the cochlear phenotypes observed in *Pax2* mutants are more severe than those observed in mice lacking *Otx1* and *Otx2*, we postulate that *Pax2* plays a key role in regulating the differential growth within the cochlear duct and thus, its proper outgrowth and coiling.
Published by Elsevier Inc.

Keywords: Inner ear; Otic vesicle; Otx; Pax; Cochlea; Hair cells; Endolymphatic duct; Stria vascularis

Introduction

The mammalian inner ear develops from an ectodermal thickening adjacent to the hindbrain that first invaginates and later pinches off from the surrounding ectoderm to form a hollow vesicle known as the otocyst. Through a largely unknown series of specifications, the simple otocyst differentiates into the complex and multifunctional inner ear. There are six major sensory organs within the mature mammalian inner ear. The five vestibular sensory organs, including the macula utriculi, macula sacculi and three cristae, detect gravity and linear and angular acceleration, respectively. The sensory organ of hearing, the organ of Corti, is housed within the cochlea.

Pax2, *Eya1* (*Eyes absent*) and *Gata3* are associated with syndromic deafness in humans. Mutations in *EYA1* and *GATA3* can lead to branchial-oto-renal (BOR) and hypoparathyroidism, sensorineural deafness, renal anomaly (HDR) syndromes, respectively (Abdelhak et al., 1997; Van Esch et al., 2000). Mutations in *PAX2* are associated with renal-coloboma syndrome, and mild sensorineural hearing loss has also been reported in some patients (Sanyanusin et al., 1995; Schimmenti et al., 1997). The etiology of these syndromes in human deafness remains unclear. In mice, all three genes are activated early and their expression persists throughout inner ear development. Consistent with these expression patterns, knockouts of these gene products severely affect the growth and morphogenesis of various components of the mouse inner ear, including the cochlear duct. These results suggest that these genes have important and multiple roles in inner ear development (Karis et al., 2001; Torres et al., 1996; Xu et al., 1999).

Three mouse models with mutations in the *Pax2* gene have been described. The *Krd* strain carries a large deletion in chromosome 19 that includes the *Pax2* locus (Keller et al., 1994). In addition, a *Pax2* knockout line (Torres et al., 1996) and a line with a frameshift mutation in *Pax2* (*Pax2*^{1Neu}) that is identical to a mutation in a human family with renal-coloboma syndrome (Favor et al., 1996) have been generated. All three mutant lines suffer kidney and eye defects. Previous studies report that the inner ears of *Pax2* knockout mice demonstrate agenesis of the cochlea and the spiral ganglion, but normal development of the vestibular portion of the inner ear (Torres et al., 1996). The *Pax2*^{1Neu} strain is missing the

* Corresponding author. NIDCD, 5 Research Ct., Room 2B34, Rockville, MD 20850. Fax: +1-301-402-5475.
E-mail address: wud@nidcd.nih.gov (D.K. Wu).

0012-1606/$ - see front matter. Published by Elsevier Inc.
doi:10.1016/j.ydbio.2004.04.024

spiral ganglion, and the ventral cochlear chamber is enlarged and continuous with the endolymphatic duct (Favor et al., 1996). In addition, in *Pax2*^{1Neu} inner ears, a distinct saccule and occasionally, the utricle and ampullae are missing.

To obtain greater insight into how a knockout of the *Pax2* gene mediates these inner ear phenotypes, especially within the cochlea, we investigated the development of the *Pax2* knockout inner ears using paint-fill and gene expression analyses. We examined the expression patterns of *Eya1* and *Gata3* in *Pax2* mutant cochlea. In the development of the *Drosophila* eye, a pax-eya-six hierarchy of gene regulation cascade has been demonstrated (Halder et al., 1998). A similar regulatory pathway involving Pax2 and *Eya1* could occur in the mammalian inner ear (Xu et al., 1999). In addition, while Pax2 and Gata3 are co-expressed in the ventral region of mouse otocyst, the expression domains of Pax2 and Gata3 in the dorsal region of the otocyst do not overlap (Lawoko-Kerali et al., 2002). The Pax2 immunoreactivity is localized medially to the Gata3 positive region. The lack of *Pax2* might result in an expansion of *Gata3* expression domain that could contribute to the resulting inner ear phenotype in *Pax2* −/− inner ears. Our results suggest that *Pax2* does not directly regulate the expression of either *Eya1* or *Gata3*. Through still unknown molecular mechanisms, the lack of *Pax2* affects the morphogenesis and tissue specification of the cochlear duct, including the organ of Corti and stria vascularis, although it does not necessarily interfere with the production of sensory hair cells.

Materials and methods

Mice and genotyping

The *Pax2* knockout line was obtained from Dr. Peter Gruss' laboratory and was maintained on a C57Bl/6 background (Torres et al., 1995). PCR was used to determine genotype. The wild-type allele for *Pax2* was identified using a forward primer (5′-AACGGTGGCAAGTTGCAGCCTCTG-3′) and a reverse primer (5′-CGCGGAGAAGGGGTCTGCTTTGCA-3′). Primers designed within the neomycin gene (forward primer: 5′ATCTCCTGTCATCTATCTCCTGTCATCTCACCTTGCT3′; reverse primer: 5′-CGGTCCGCCACACCCAGC-3′) were used to identify the mutant allele.

Phenotypic analysis and in situ hybridization

Paint-fill analysis of inner ear gross anatomy was performed according to Morsli et al. (1998). Cryostat tissue sections were processed for in situ hybridization as described (Morsli et al., 1998). A total of 35 *Pax2* homozygous embryos was used for gene expression analysis: 11 between 9.5 and 10.5 dpc, 8 between 11.5 and 12.5 dpc and 18 at 15.5 dpc. RNA probes for *Bone morphogenetic protein 4* (*Bmp4*), *Lunatic fringe* (*Lfng*), *Orthodenticle 2* (*Otx2*), *Tyrosinase-related protein 2* (*Trp2*) and *Neurofilament protein 68 kDa* (*NF68*) were previously described (Morsli et al., 1999). RNA probes for *Eye-absent 1* (*Eya1*) (Xu et al., 1997), *Gata3* (Karis et al., 2001), *Pax2* (Dressler et al., 1990), *Pendrin* (*Pnd*) (Everett et al., 1999), *Myosin XV* (*Myo15a*) (Anderson et al., 2000), *NeuroD1* (Ma et al., 1998) and *Retinaldehyde dehydrogenase enzyme 2* (*Raldh2*) (Zhao et al., 1996) were prepared according to cited references.

Apoptosis and proliferation assays

Apoptotic cells were identified using terminal dUTP nick-end labeling (TUNEL) method (ApopTag). Cryostat sections were treated three times with a 2:1 volume of ethanol/acetic acid solution for 10 min each before following the manufacturer's protocol.

To detect proliferating cells, pregnant mice were injected intraperitoneally with a labeling reagent containing 10 mM 5-bromo-2′-deoxyuridine (BrdU) and 1 mM 5-fluoro-2′-deoxyuridine (Cell proliferation Kit, Amersham) at a concentration of 0.03 ml/gm body weight 2 h before sacrificing. Harvested embryos were fixed with 4% paraformaldehyde and processed for cryosectioning. Frozen sections were pretreated with proteinase K (5 μg/ml) for 2 min before incubating with a 50% formamide solution containing 5× SSC (saline sodium citrate) and 1% SDS for 30 min at 65°C. Anti-BrdU staining was performed according to manufacturer's procedures.

Results

Paint-fill analysis of Pax2 −/− mutants

We used the paint-fill technique to evaluate the gross anatomy of the inner ears from a total of 5 *Pax2* homozygous embryos at 12 dpc and 17 embryos between 14.5 and 15.5 dpc. In wild-type embryos at 12 dpc, three separate inner ear compartments can be distinguished: a medially positioned endolymphatic duct, a dorsal vestibular component containing the vertical and horizontal canal pouches (Figs. 1A, C, vp, hp) and a ventral auditory component, the cochlear duct (Figs. 1A, C, cd). In 12 dpc mutant embryos, the vestibular component appears normal in the mutants (Fig. 1B). The resorption domain (rd) shown in Fig. 1B is normal for this age. However, the endolymphatic duct is malformed and is either broader (Fig. 1B, $n = 2$), or smaller than normal (Fig. 1D, $n = 3$). The cochlear region is wider than normal and shows a stunted ventral extension (Figs. 1B, D).

By 15.5 dpc, the gross morphogenesis of the inner ear is nearly complete except for the cochlear duct, which has not yet acquired its full 1.75 turns (Fig. 2A). Mild (Figs. 2B, E) and more severe (Figs. 2C, F) mutant inner ear phenotypes

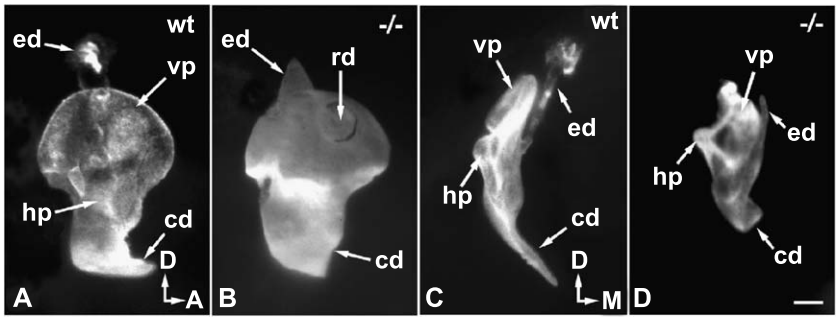

Fig. 1. Paint-filled inner ears of wild-type and *Pax2* mutants at 12 dpc. Lateral (A, B) and anterior (C, D) views of wild-type (wt) (A, C) and *Pax2* homozygous knockout (− / −) (B, D) inner ears. (A, C) A wt inner ear consists of three parts: a medial ed, a dorsal vestibular and ventral cochlear component (cd). The vestibular component consists of vertical and horizontal canal pouches. In mutant inner ears (B), the ed is either short and broad, or smaller (D) than the wt. The primordial cochlear duct fails to extend in − / − embryos (B, D), but the resorption domain in B is normal for this age. Abbreviations: cd, cochlear duct; ed, endolymphatic duct; hp, horizontal canal pouch; vp, vertical canal pouch; rd, resorption domain. Orientation arrows: A, anterior; D, dorsal; M, medial. Scale bar = 100 μm.

are shown in both lateral (Figs. 2B, C) and anterior (Figs. 2E, F) views. Due to exencephaly, most of the *Pax2* mutant inner ears are mis-oriented with the semicircular canals laterally displaced and the cochlear duct medially displaced (Fig. 2C, $n = 15/17$). Despite the lateral displacement of the three ampullae and semicircular canals, these structures formed in all *Pax2* −/− embryos examined. However, the diameter of the semicircular canals (asc, lsc and psc) and the size of the ampullae are sometimes smaller (Fig. 2B, $n = 5$) or slightly larger (Fig. 2C, $n = 6$) than normal.

The malformation in the cochlear duct is quite obvious with less than a single turn (Figs. 2B, E, F). The mutant cochlear duct is continuous with the endolymphatic duct, a feature that is also similar in the wild-type inner ear (Cantos

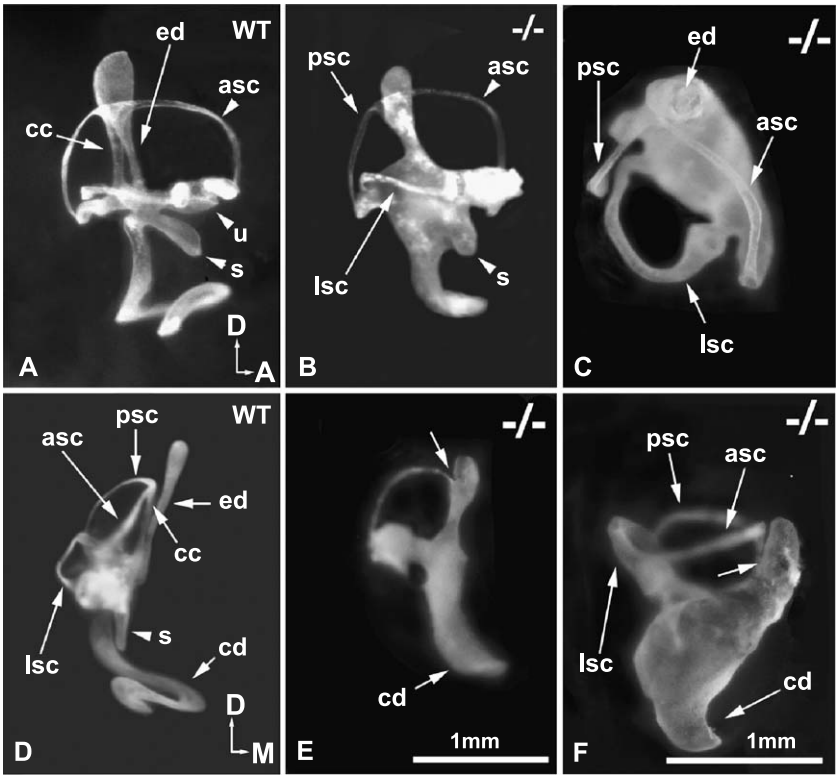

Fig. 2. Paint-filled inner ears of wild-type and *Pax2* mutants at 15.5 dpc. A, B and C are lateral views and D, E and F are anterior views of wild-type (wt) or mutant inner ears. (A, D) A wt inner ear showing a fairly mature morphology. (B, E) A *Pax2* homozygous inner ear with a less severe phenotype than the one in C and F. The cochlea is shortened, and the common crus and the ed are fused. The semicircular canals are slightly thinner than wt. (C, F) A more severe form of a *Pax2* mutant inner ear with semicircular canals displaced laterally due to exencephaly. The diameter of the semicircular canals is larger than wt, and the cochlea is shortened. However, the fusion between the common crus and the ed (arrow) is at a more ventral location than the specimen shown in E. Abbreviations: asc, anterior semicircular canal; cc, common crus; cd, cochlear duct; ed, endolymphatic duct; lsc, lateral semicircular canal; psc, posterior semicircular canal; s, saccule; u, utricle. Orientation arrows: A, anterior; D, dorsal; M, medial.

et al., 2000), except the normal restrictions between the saccule and the cochlear duct, and the saccule and the endolymphatic duct are missing in the mutants (Figs. 2E, F). A distinct compartment for the saccule is only evident in three specimens (Fig. 2B, s). However, the endolymphatic duct and the common crus are invariably fused in all specimens examined. In most cases, the two structures are indistinguishable from each other (Fig. 2E, arrow, $n = 13$). In others, the fusion occurred near the base of the common crus and a small but separate endolymphatic duct can be identified (Fig. 2F, arrow, $n = 3$). Although we observed these variations in the phenotype between different specimens, the right and left ears of the same embryo are always similar ($n = 13$).

Relationship of Pax2 expression domains with presumptive sensory patches

To better understand the role of *Pax2* in inner ear development, we first compared the pattern of *Pax2* gene expression with the expression patterns of genes such as *Bmp4* and *Lfng* that are expressed in specific presumptive sensory tissues (Morsli et al., 1998). The expression of *Pax2* in the mouse inner ear has been described in several publications (Nornes et al., 1990; Puschel et al., 1992; Rinkwitz-Brandt et al., 1995, 1996). A more detailed account of *Pax2* expression pattern in the developing mouse inner ear was reported by Lawoko-Kerali et al. (2002), using an antibody against the Pax2 protein. They described the presence of *Pax2* immunoreactivity in the medial region of the newly formed otocyst. As the otocyst develops into various components, *Pax2* is expressed in the endolymphatic duct, in the hair cells of all differentiating sensory epithelia and in some non-sensory regions (Lawoko-Kerali et al., 2002).

In a newly formed otocyst, *Lfng* is broadly expressed in the antero-ventral lateral and medial regions of the tear drop-shaped structure. This *Lfng* positive region is thought to encompass the neurogenic region as well as the presumptive sensory regions for the utricle, saccule and cochlea (Morsli et al., 1998). At 10.5 dpc, *Pax2* expression only overlaps with the *Lfng* domain in the medial but not the lateral region (most likely the neurogenic region, Figs. 3A, B, brackets) of the otocyst. Even though *Pax2* expression domain is mostly medial, it expands laterally in the more posterior regions of the otocyst (Figs. 3C, D, arrowheads). By 11.5 dpc, many neuroblasts have already delaminated from the otic epithelium. Two separate *Lfng* expression domains are present in the inner ear, a dorsal domain that corresponds to the macula of the utricle (Fig. 3H, mu) and a more ventral domain that corresponds to the macula of the saccule and organ of Corti (Fig. 3J, msc; Morsli et al., 1998). *Pax2* expression overlaps only partially with the macula of the utricle (Figs. 3G, H, bracket). No obvious overlap of *Pax2* expression with the sensory regions for the saccule and cochlea was observed (Figs. 3I, J). At that level, *Pax2* is mostly expressed in the posterior region of the inner ear.

Bmp4 is expressed in all three presumptive cristae of the mouse inner ear (Morsli et al., 1998). Fig. 3F illustrates *Bmp4* expression in the presumptive posterior crista (pc) as well as the anterior and lateral cristae, which are still connected at this age (Figs. 3E, F, as). The *Pax2* expression domain does not overlap with any of the presumptive cristae at this stage. In addition, *Pax2* is expressed in a small region anterior to the posterior crista (Fig. 3E, arrow), a region that most likely corresponds to the base of the common crus in a mature inner ear.

At 15.5 dpc, *Pax2* expression is not detected in most of the sensory regions except in the medial region of the macula utriculi (Figs. 4K, L, arrowheads) and the posterior region of the macula sacculi (Figs. 3O, P, bracket). In the cochlea, *Pax2* expression is robust in the stria vascularis region (Fig. 3M, sv) but below detection in the *Lfng* positive, sensory region (Figs. 3M, N). In addition, *Pax2* is expressed in other non-sensory regions such as the roof of the utricle (Fig. 3K, arrows), endolymphatic duct and lateral region of the common crus (Fig. 3O, ed, cc). The reported immunoreactivity of *Pax2* in sensory hair cells of all sensory regions (Lawoko-Kerali et al., 2002) is much more evident by postnatal day 1 (P1) using in situ hybridization (Figs. 3Q, S). The identity of the *Pax2* positive sensory hair cells in the organ of Corti was confirmed by probing an adjacent section for transcripts of a hair cell marker, *Myo15a* (Fig. 3R; Anderson et al., 2000).

Sensory organ and ganglion development in Pax2 mutants

Previous reports noted the absence of the spiral ganglion in *Pax2* knockout mice (Torres et al., 1996) and massive cell death associated with the ganglion in the $Pax2^{1neu}$ strain at 14.5 dpc (Favor et al., 1996). We examined the vestibular and spiral ganglia in the *Pax2* −/− mutants at 15.5 dpc using RNA probes against *NF68*, *Eya1* and *Gata3* transcripts. *NF68* and *Eya1* are expressed in both vestibular and spiral ganglia, whereas *Gata3* is only expressed in the spiral ganglion (Kalatzis et al., 1998; Karis et al., 2001). We observed a decrease in the size of the vestibular ganglion in some mutant specimens, compared to wild-type (Figs. 4A, B, vg; $n = 5/8$). However, most of the mutant inner ears are lacking the spiral ganglion (Figs. 4C, D, sg; $n = 2/8$).

We further examined whether the lack of neurons in the ganglia is due to abnormal delamination of neuroblasts from the otic epithelium at the otocyst stage. At 10.5 dpc, there is no obvious change in the neurogenic/sensory competent region in the *Pax2* mutants, based on the expression pattern of *Lfng* (Figs. 4E, G). As marked by the expression domain of *NeuroD1* (Kim et al., 2001; Liu et al., 2000), the neurogenic region also appears normal in the mutants (Figs. 4F, H). Also, no obvious change in the size of the ganglion is observed at 11.5 dpc (Figs. 4I, J, arrowheads), including the spiral ganglion component as indicated by the expres-

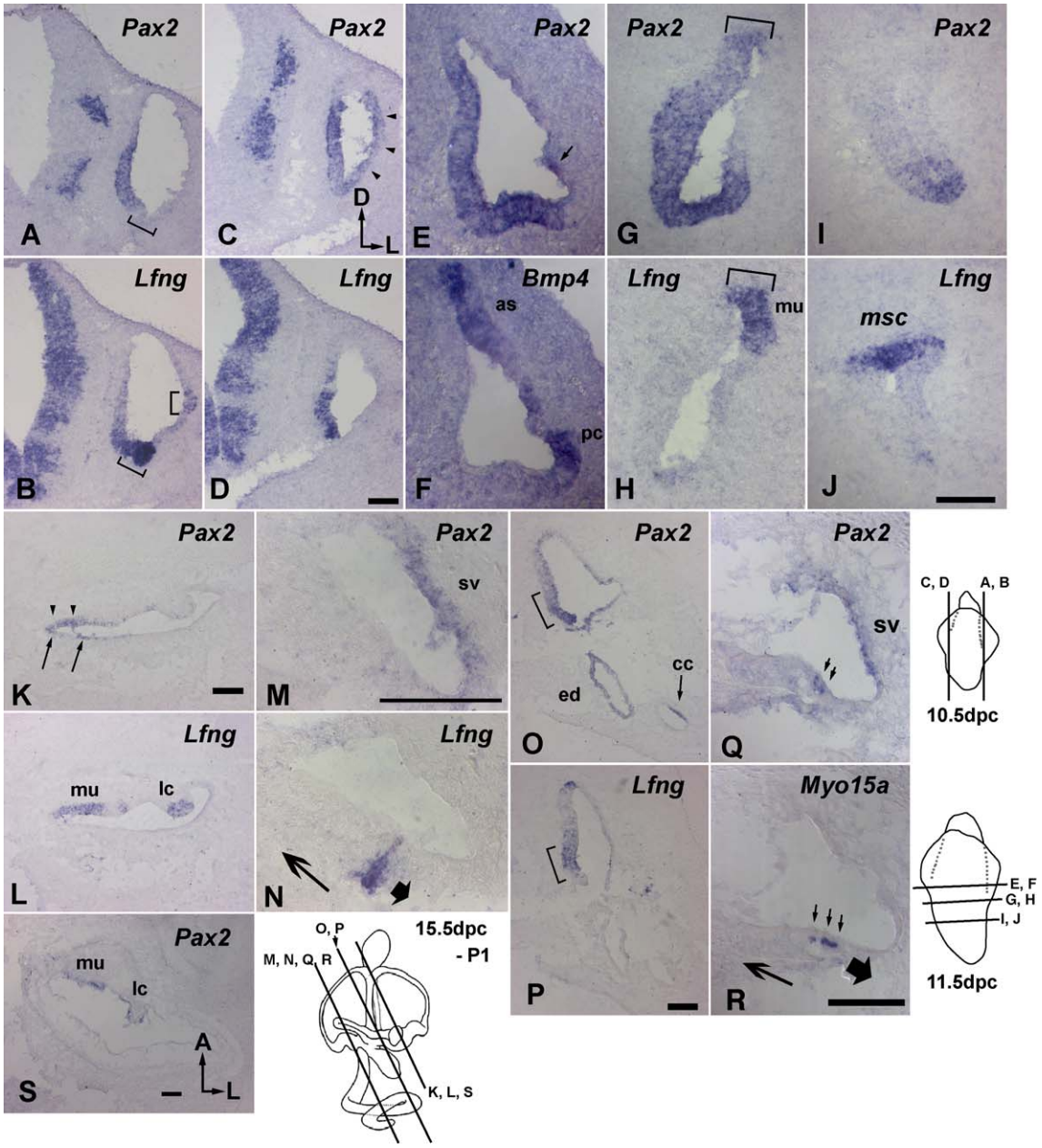

Fig. 3. Normal expression of *Pax2* in the developing wild-type mouse inner ear. Cryostat sections of inner ear at 10.5 dpc (A–D), 11.5 dpc (E–J), 15.5 dpc (K–P), and P1 (Q–S). A, C, E, G, I, K, M, O and Q are 12 μm adjacent sections of B, D, F, H, J, L, N, P and R, respectively. The approximate levels of sections are indicated in the respective schematic diagrams. (A, B) At 10.5 dpc, *Pax2* (A) expression domain overlaps with the *Lfng* (B) expression domain medially but not laterally (brackets). In posterior sections, *Pax2* (C) still overlaps with *Lfng* (D) medially, but *Pax2* is also expressed on the lateral side (arrowheads). (E, F) At 11.5 dpc, *Pax2* (E) is not expressed in the *Bmp4* positive, presumptive cristae (F), but is expressed in the small region located anterior to the posterior crista (arrow). (G, H) *Pax2* (G) expression overlaps partially with the *Lfng* positive, macula utriculi (H, mu). Brackets in G and H mark the region of overlap between *Pax2* and *Lfng*. (I, J) *Pax2* (I) expression is predominantly in the posterior pole at the level of the macula sacculi and cochlea (J, msc). (K, L) At 15.5 dpc, *Pax2* (K) is expressed in the medial sensory (arrowheads) and non-sensory (arrows) regions of the cochlea. *Pax2* expression within the cristae and the rest of the macula utriculi is below the level of detection. (M, N) *Pax2* (M) is expressed in the stria vascularis (sv) and not in the *Lfng* positive sensory region of the cochlea (N). (O, P) *Pax2* (O) is expressed in the medial saccule, the ed and lateral region of the common crus. Brackets in O and P mark the region of overlap in the macula sacculi between *Pax2* and *Lfng*. (Q, R) At P1, *Pax2* (Q) is expressed in the stria vascularis and sensory hair cells (arrows) in the organ of Corti that are also positive for *Myo15a* (R). One inner and three outer hair cells can be discerned in R. A long arrow points toward the neural side (inner hair cell side), whereas the short block arrow points toward the abneural side (outer hair cell side) of the cochlear duct in both N and R. (S) *Pax2* is expressed in sensory hair cells of the lateral crista and macula utriculi. Abbreviations: as, anterior streak containing both anterior and lateral cristae; cc, common crus; ed, endolymphatic duct; lc, lateral crista; msc, macula sacculi and organ of corti; mu, macula utriculi; pc, posterior crista; sv, stria vascularis. Orientation arrows: A, Anterior; D, Dorsal; L, Lateral. Scale bars = 100 μm; D applies to A–C; J applies to E–I; K applies to L; M applies to N; P applies to O; R applies to Q.

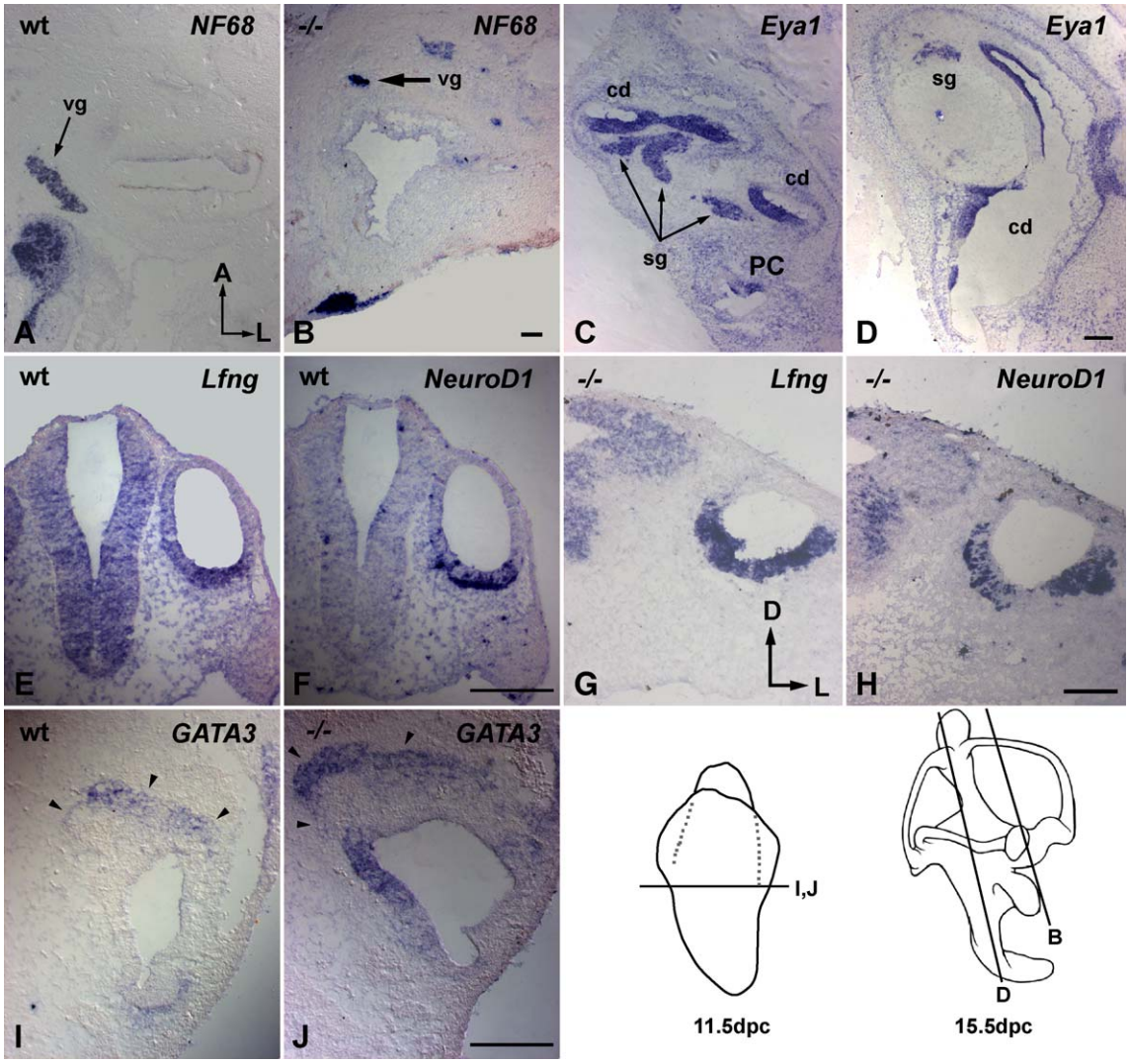

Fig. 4. Development of the vestibular and spiral ganglia in *Pax2* mutants. Wild-type (A, C) and *Pax2* −/− (B, D) inner ears at 15.5 dpc. *NF68* (A, B) and *Eya1* (C, D) expression patterns in the vestibular (vg, A, B) and spiral (sg, C, D) ganglia of wild-type (A, C) and *Pax2* homozygous (B, D) inner ears at 15.5 dpc, respectively. (E–H) Expression patterns of *Lfng* (E, G) and *NeuroD1* (F, H) in wild-type (E, F) and *Pax2* −/− (G, H) inner ears at 10.5 dpc. E and G are 12 μm adjacent sections of F and H, respectively. *NeuroD1* positive cells are within the *Lfng* positive domain for both wild-type and mutants. (I, J) *Gata3* expression in the spiral ganglion component of the delaminated neuroblasts in wild-type (I) and mutant (J) inner ears at 11.5 dpc. Arrowheads point to the rim of the neuroblast cluster. Refer to schematic diagrams in Fig. 3 for planes of sections for A, C and E–H. Scale bars = 100 μm.

sion of *Gata3*. These results indicate that the loss of sensory neurons in vestibular and spiral ganglia in *Pax2* −/− mutants occurs after the delamination process, presumably due to a lack of neurotrophin support from the macula sacculi and organ of Corti, respectively.

We also examined the formation of sensory patches in *Pax2* mutants at 15.5 dpc. On the basis of the expression patterns of *Lfng* and *Myo15a* (Figs. 5A, D, lc and mu; $n = 12$), all three cristae and the macula utriculi are invariably present and contain nascent hair cells in *Pax2* homozygous inner ears examined at 15.5 dpc. A well-defined saccule is not evident in most of the specimens following paint-fill. However, a distinct but smaller macula sacculi can be identified within the enlarged ventral chamber in more than half of the mutants processed for gene expression analysis (Figs. 5B, E, ms; $n = 8$ out of 12). More ventrally, only a few scattered sensory patches can be found on the medial side (Figs. 5B, C, arrowheads). The association of these sensory patches with genes normally expressed in the cochlea suggests that they are part of a rudimentary organ of Corti (see below). In addition, some of these sensory patches also express the hair cell marker, *Myo15a* (Figs. 5E, F).

Cell death in cochlear duct of Pax2 mutants

To better elucidate the mechanisms underlying the cochlear duct phenotype in *Pax2* mutants, we performed cell proliferation and TUNEL assays. Because paint-fill analysis indicates that the cochlear phenotype in *Pax2* mutants is already evident at 12 dpc, we evaluated cell proliferation

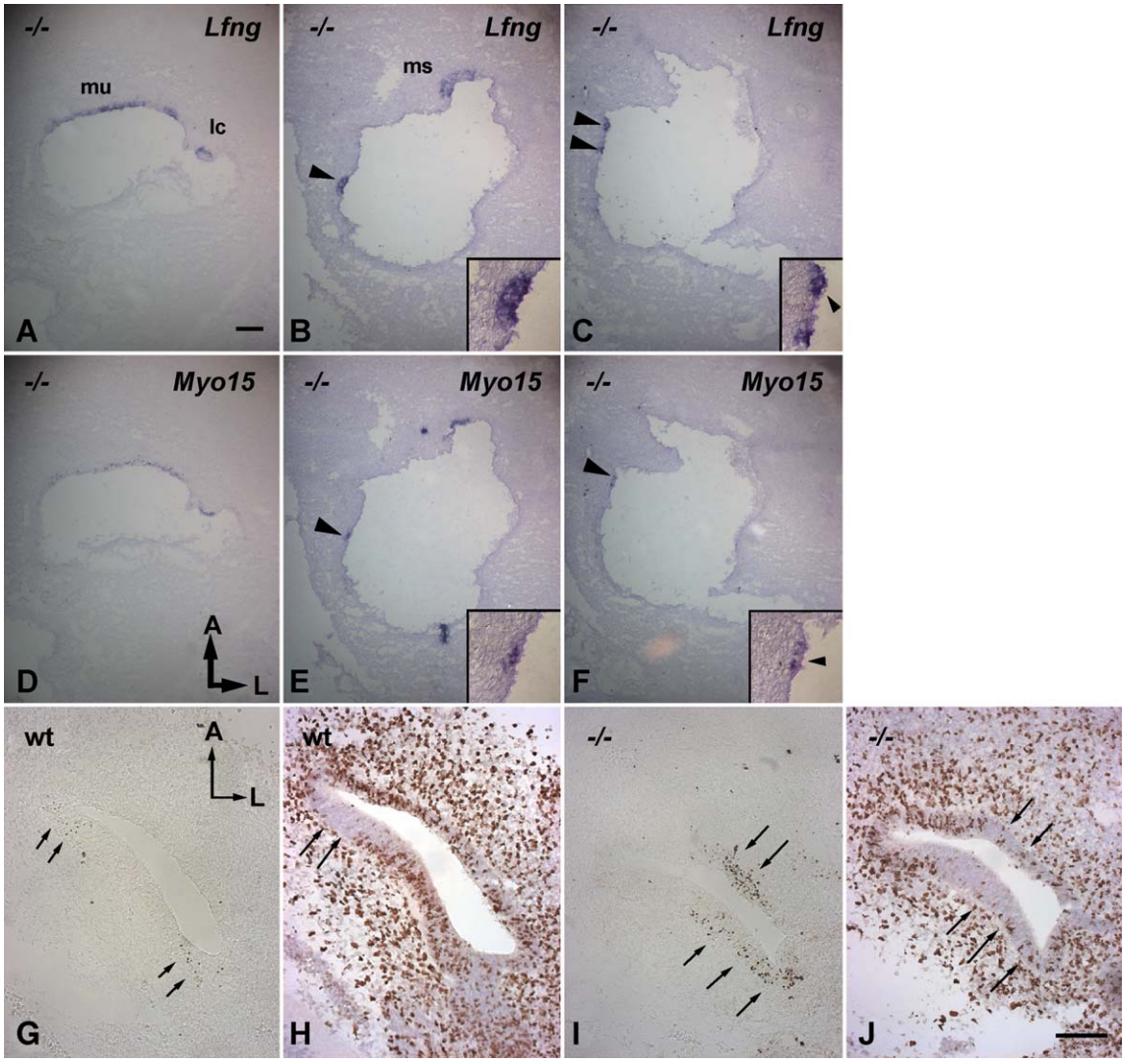

Fig. 5. Development of sensory patches and cochlear duct in *Pax2* mutants. A, B and C are 12 μm adjacent sections of D, E and F from the same *Pax2* mutant inner ear in a dorsal to ventral direction at 15.5 dpc. (A) *Lfng* and (D) *Myo15a* expression patterns in the lateral crista (lc) and macula utriculi (mu). Expression patterns of *Lfng* (B) and *Myo15a* (E) in the macula sacculi (ms). Arrowheads in B, C, E and F point to the scattered sensory patches located in the cochlea. Inserts in B, C, E and F show an overlap between *Myo15a* and *Lfng* expression domains. Only one of the *Lfng* positive domains in C is also positive for *Myo15a* expression (arrowheads in insert of C and F). Refer to the 15.5 dpc schematic diagram in Fig. 4 for approximate planes of sections. (G–J) Cell proliferation and apoptosis in the cochlea of *Pax2* mutants at 11.5 dpc. Brightfield micrographs showing apoptotic (G, I) and BrdU (H, J) labeled nuclei as brown profiles. Panels in H and J have been counterstained with hematoxylin. (G, H) Adjacent wild-type cochlear sections processed for TUNEL (G) and anti-BrdU staining (H). (G) Two small regions of apoptosis are evident in the wild-type cochlea (arrows). The anterior region of apoptosis overlaps with a cold spot of proliferation in H. (I, J) Adjacent cochlear sections from *Pax2* −/− ears processed for TUNEL (I) and anti-BrdU staining (J). (I) Extensive apoptosis is observed in the lateral and postero-medial regions of the mutant cochlea (arrows). A concomitant reduction in BrdU positive cells is observed in the same regions (J, arrows). Scale bars = 100 μm; A applies to B–F; J applies to G–I.

and programmed cell death from 10.5 to 12.5 dpc. We did not observe a consistent change in either parameter at 10.5 dpc ($n = 3$). However at 11.5 dpc, we observed an increase in TUNEL positive cells and a decrease in BrdU positive cells. In the normal inner ear, there are some apoptotic cells in the anterior and posterior regions of the cochlea (Fig. 5G, arrows). The TUNEL positive cells in the anterior region of the cochlear duct are located in a low proliferation zone (Fig. 5H, arrows). Except for this low proliferation zone (Fig. 5H, arrows), the epithelial cells are fairly uniformly labeled for BrdU, including cells in the region that normally express *Pax2* (compare Fig. 5H with Figs. 3G and 3I). In *Pax2* mutants, an increase in programmed cell death is present in the lateral as well as postero-medial regions of the cochlear duct (Fig. 5I, arrows, $n = 4$), a region that normally expresses *Pax2* (Figs. 3G, I). A concomitant decrease in BrdU-labeled cells is also present in the same regions undergoing rapid cell death (Fig. 5J, arrows, $n = 3$). By 12.5 dpc, apoptosis within the otic epithelia is greatly reduced in the mutants (data not shown).

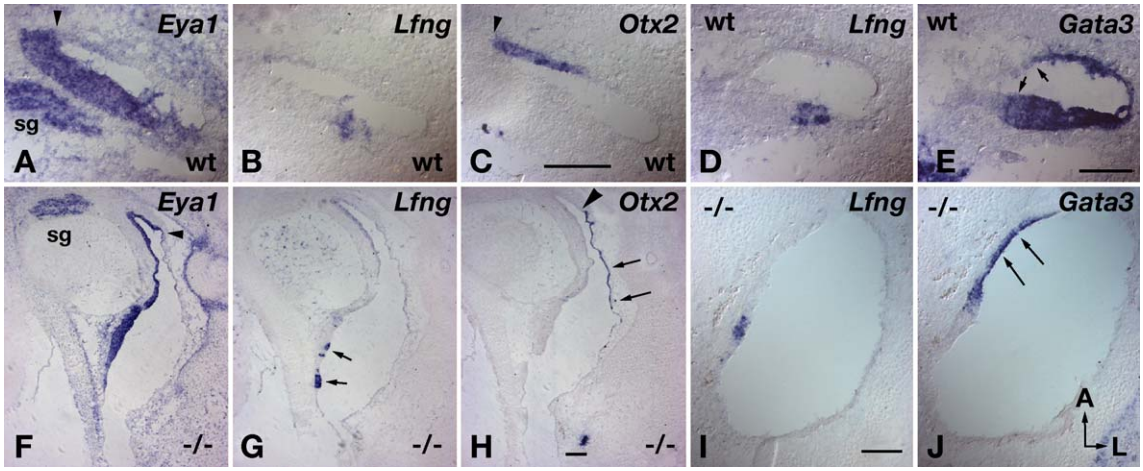

Fig. 6. Gene expression patterns of *Eya1*, *Otx2* and *Gata3* in the cochlea of *Pax2* mutants at 15.5 dpc. Expression patterns of *Eya1*(A), *Lfng* (B) and *Otx2* (C) in adjacent sections of wild-type cochlea at 15.5 dpc. (A) *Eya1* is expressed in the posterior wall of the cochlear duct. (B) *Lfng* is expressed in the sensory region of the cochlea. (C) *Otx2* is expressed in the Reissner's membrane and its expression domain abuts the expression domain of *Eya1* (arrrowhead). (D, E) *Lfng* (D) and *Gata3* (E) expression patterns in adjacent sections of wild-type cochlea. Arrows in E point to the borders of *Gata3* domain in the cochlear duct. Expression patterns of *Eya1* (F), *Lfng* (G) and *Otx2* (H, arrows) in adjacent sections of *Pax2* mutant cochlea at 15.5 dpc. The relationship of *Eya1* and *Otx2* expression domains is maintained in *Pax2* mutants (arrowheads in F, H). Arrows in G point to *Lfng* positive sensory patches. (I, J) Expression patterns of *Lfng* (I) and *Gata3* (I) in adjacent sections of *Pax2* mutants. Arrows in J point to the *Gata3* positive domain anterior to the *Lfng* positive, sensory region (I). Abbreviation: sg, spiral ganglion. Orientation arrows: A, anterior; L, lateral. All cross sections of wild-type cochlea are oriented with neural side toward the left. Refer to the 15.5 dpc schematic diagram in Fig. 4 for planes of sections for mutant embryos. Scale bars = 100 μm; C applies to A and B; E applies to D; H applies to F and G; I applies to J.

Gene expression changes in the cochlear duct

To determine the consequences of such extensive cell death on various regions of cochlear duct development, we examined the expression patterns of several region-specific genes. Despite the hierarchy of pax-eya-six regulation that has been shown in other organs, both *Eya1* and *Six1* expression patterns appear normal in *Pax2* −/− otocysts (Zheng et al., 2003). We further examined if *Eya1* expression is affected in the developing cochlea of the *Pax2* mutants. Normally, *Eya1* is expressed in the spiral ganglion and the posterior wall of the cochlear duct that includes the organ of Corti (Figs. 6A, B; Kalatzis et al., 1998), whereas *Otx2* is a marker for the Reissner's membrane (Fig. 6C; Morsli et al., 1999). The two expression domains abut each other toward the neural (ganglion) side of the cochlear duct (Figs. 6A, C; arrowhead). In the *Pax2* mutants, the *Eya1* expression domain remains associated with the *Lfng* positive sensory domain, except both domains are found medially (Figs. 6F, G) rather than in the normal posterior position by this stage (Figs. 6A, B). However, there is no obvious difference in the relationship of *Eya1* and *Otx2* expression patterns, the two domains remain juxtaposed (Figs. 6F, H, arrowhead).

Gata3 is normally broadly expressed in the cochlear duct at this stage, with an expression domain spanning from the greater epithelial ridge to the stria vascularis and includes the sensory region (Figs. 6D, E; Karis et al., 2001). The *Gata3* expression domain, though always present, is often reduced in the *Pax2* mutants ($n = 5$). The specimen in Fig. 6J shows *Gata3* expression localized anterior to the *Lfng* positive sensory domain but not posterior to it (Figs. 6I, J, arrows).

Because *Pax2* is primarily expressed toward the abneural side (beyond the outer hair cells region) of the cochlear duct (Figs. 3I, M, N, block arrow), we further examined genes specifically expressed between the outer hair cells and stria vascularis regions. In a normal cochlea, *Bmp4* is expressed in the Hensen's and Claudius' cells adjacent to the outer hair cells (Figs. 7A, B; Morsli et al., 1998). *Pnd* is expressed in

Fig. 7. Gene expression patterns in the cochlea of *Pax2* −/− mutants at 15.5 dpc. A, B and C are 12 μm adjacent sections of wild-type cochlea. (A) *Lfng* positive, sensory region, (B) *Bmp4* positive, Hensen's and Claudius' cell regions, and (C) *Pnd* positive, external sulcus region in wild-type cochlea. (D, E) Adjacent sections showing the *Lfng* positive sensory region (D, arrowheads) overlaps with the *Bmp4* positive region (E, arrowheads) in the mutant cochlea. (F, G) Adjacent sections showing *Lfng* positive sensory region (F, arrow) overlaps with *Pnd* positive region (G, arrows) in mutants. An arrowhead in G is pointing to normal *Pnd* expression found between the lateral crista and macula utriculi. (H–J) Adjacent sections of wild-type cochlea. (H) *Lfng* is expressed in the sensory region. (I) *Raldh2* is expressed in the stria vascularis (arrows) and mesenchymal cells adjacent to the Reissner's membrane (arrowheads). (J) *Trp2* is expressed in melanocytes within the stria vascularis. (K–M) Adjacent sections of *Pax2* mutants. The *Lfng* positive sensory region (K) is encompassed within the *Raldh2* (L) and *Trp2* (M) positive regions. Inserts in K, L and M are higher magnification of tissues outlined within the box, and show that *Raldh2* and *Trp2* positive cells are spanning both sides of the *Lfng* positive, sensory domain (arrow). (L) Arrowheads point to *Raldh2* expression in mesenchymal cells associated with the Reissner's membrane. Arrows in M point to the *Trp2* positive melanocytes in aberrant positions that are not associated with the *Raldh2* positive epithelial region. Abbreviations: lc, lateral crista; ms, macula sacculi; mu, macula utriculi. Orientation arrows: A, anterior; L, lateral. Neural side of wild-type cochlea is toward the left. Scale bars = 100 μm; A applies to B–C; G applies to D–F; I applies to H and J; L applies to K and M.

the outer sulcus region, even further away from the outer hair cell region (Fig. 7C; Everett et al., 1999; Royaux et al., 2003). In the *Pax2* −/− inner ears, *Bmp4* positive cells are intermingled within the *Lfng* positive domain (Figs. 7D, E, arrowheads). However, the expression of *Bmp4* in the cristae is normal (data not shown). *Pnd* expression also co-localizes with the *Lfng* positive sensory domain in the cochlear duct (Figs. 7F, G; arrows). The normal expression of *Pnd* between the lateral crista and the macula utriculi, however, is unaffected in *Pax2* mutants (Fig. 7G, arrow-

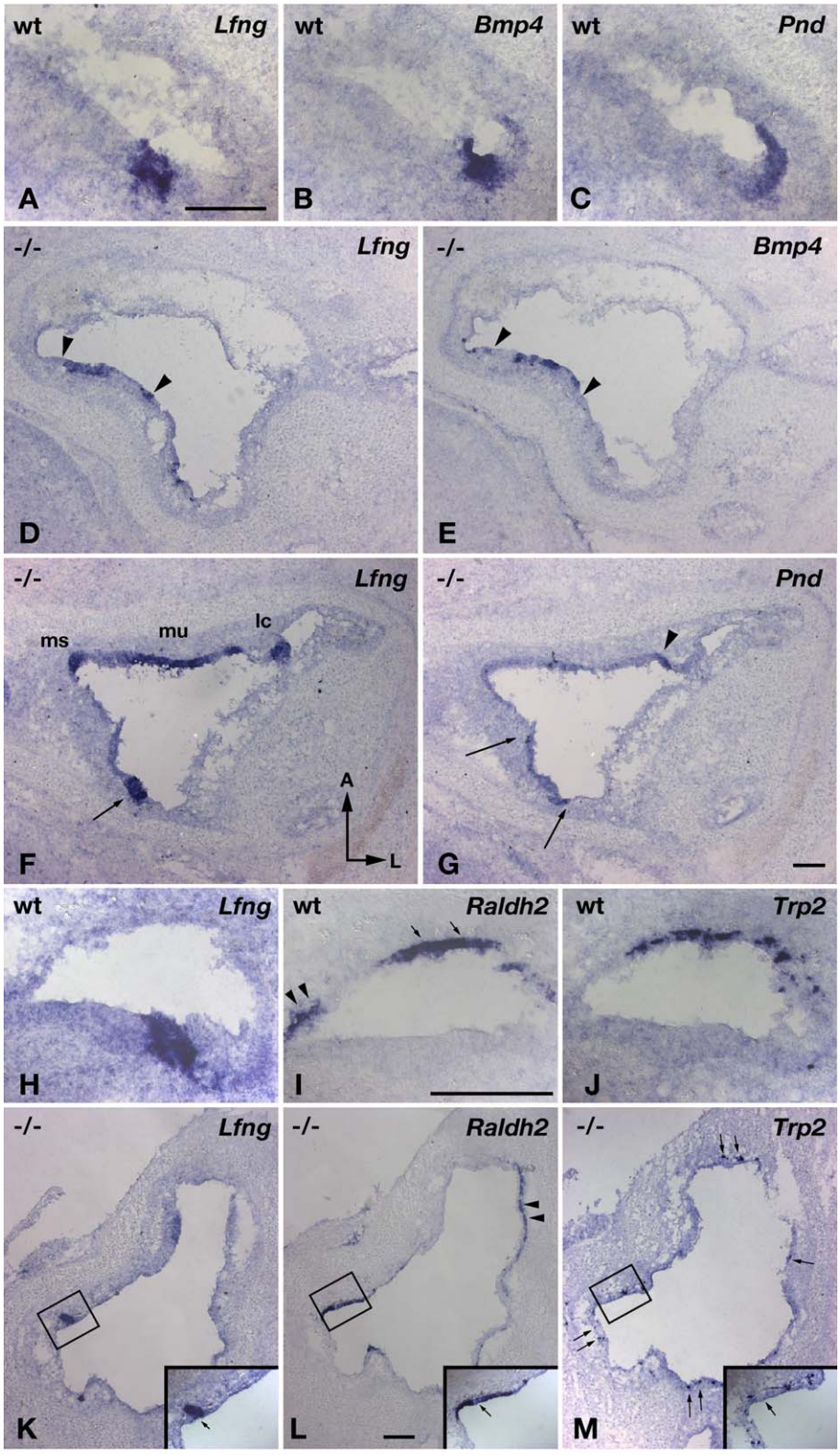

head; Everett et al., 1999). Taken together, these results suggest that the expression of *Bmp4* or *Pnd* in the inner ear is not dependent on *Pax2*, but the lack of *Pax2* affects the development of cells expressing *Bmp4* and *Pnd* in the cochlea.

In addition, *Raldh2* is not expressed in the *Lfng* positive sensory region (Fig. 7H) but is expressed in the stria vascularis (Fig. 7I, arrows) as well as the mesenchymal cells adjacent to the Reissner's membrane (Fig. 7I, arrowheads; Romand et al., 2001). *Trp2*, a marker for the neural crest-derived melanocytes, is co-localized with *Raldh2* in the stria vascularis region (Fig. 7J; Steel et al., 1992). In the *Pax2* mutants, the location of the *Raldh2* positive, epithelial region overlaps with some of the *Lfng* positive, sensory regions instead (Figs. 7K, L). However, most of the *Raldh2* positive mesenchymal cells (Fig. 7L, arrowheads) are associated with the lateral region of the cochlear duct that is *Otx2* positive (Fig. 6H, arrows), similar to wild-type (Figs. 6C and 7I; Morsli et al., 1999). In addition, in the *Pax2* mutants, *Trp2* positive cells are no longer restricted to the *Raldh2* positive epithelial region. Instead, *Trp2* positive cells are scattered in different areas of the cochlear duct (Fig. 7M, arrows). Some *Trp2* positive cells are located anterior as well as posterior to some of the sensory patches (Figs. 7K, M), similar to patterns observed for *Bmp4*, *Pnd* and *Raldh2*.

Taken together, these results indicate that the tissue specification of the cochlear duct is affected in the *Pax2* mutants, in particular the posterior and lateral walls of the cochlear duct. The lack of *Pax2* causes cell death and arrest of cochlear development around 11.5 dpc. We reasoned that apoptosis is a consequence of gene expression changes due to absence of Pax2 activity most likely before 11.5 dpc. However, expression patterns of the genes tested thus far including *Gata3*, *Gbx2*, *Foxg1*, *Eya1*, *Lfng* and *NeuroD* are all normal in the mutants at the otocyst stage (data not shown).

Gene expression in endolymphatic duct of Pax2 −/− mutants

The endolymphatic duct/sac is important for maintaining the fluid homeostasis of the membranous labyrinth. Improper development or differentiation of the endolymphatic duct/sac has been shown to disrupt this process and result in swelling of the membranous labyrinth (Everett et al., 2001; Hulander et al., 2003). Therefore, the variability in the sizes of the semicircular canals as well as the cochlear duct could be due to a functionally compromised endolymphatic duct/sac in the mutants. In normal inner ears, *Delta*, *Serrate* and *Pnd* are expressed in subsets of cells within the endolymphatic sac (Figs. 8A–C; Everett et al., 1999; Morrison et al., 1999). We examined the mutant inner ears for these transcripts and found that some specimens do express these genes in the most apical region of the endolymphatic duct (Figs. 8D–F, n = 2/4), resembling those cells found nor-

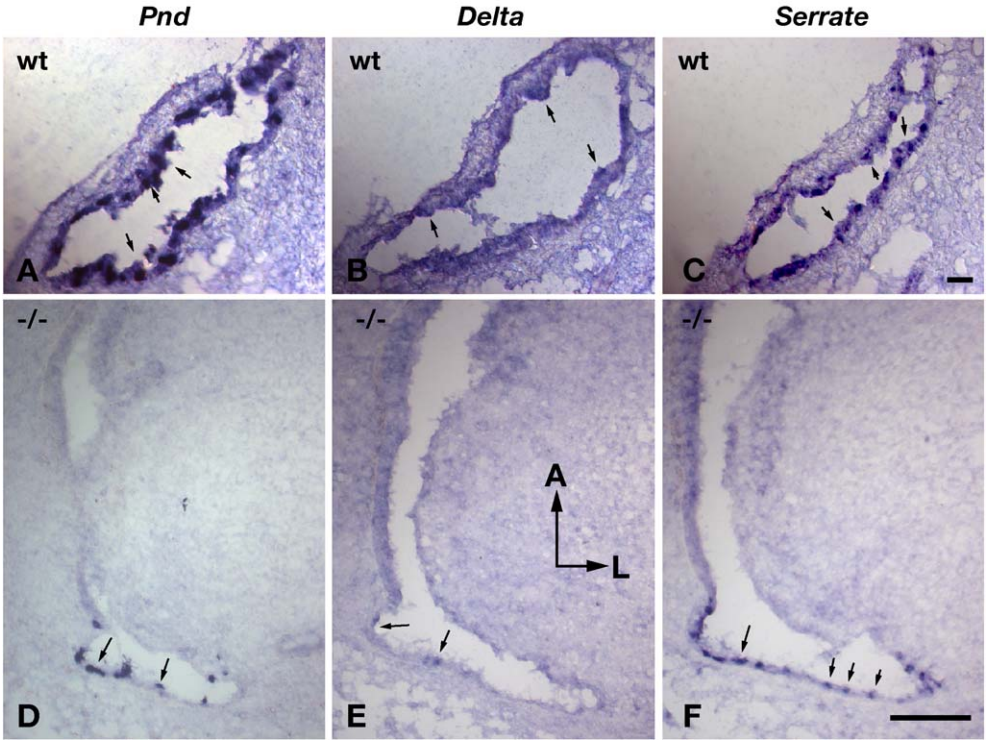

Fig. 8. Gene expression patterns in the endolymphatic duct of *Pax2* mutants. Expression patterns of *Pnd* (A, D), *Delta* (B, E), and *Serrate* (C, F) in the endolymphatic duct of wild-type (A, B, C) and *Pax2* homozygous (D, E, F) inner ears at 15.5 dpc. Arrows in D, E and F point to positive cells in the most distal region of the endolymphatic duct that resemble the wild-type pattern. Orientation arrows: A, anterior; L, lateral. Scale bar = 100 μm.

mally in the endolymphatic sac (Everett et al., 1999; Morrison et al., 1999). These results suggest that despite the malformations of the endolymphatic duct and sac in *Pax2* mutants, some progression of cellular differentiation occurred.

Discussion

Cell autonomous role of Pax2 in inner ear development

Transcription factors are thought to be cell autonomous because a transcription factor activates specific gene transcription within a given cell. However, it is conceivable that a given transcription factor could have indirect non-cell autonomous roles if one of its downstream genes encodes a signaling molecule that mediates functions in neighboring cells. Indeed, *Pax2* has a non-cell autonomous role in kidney development. *Pax2* expressed in the metanephric mesenchyme induces glia cell-derived neurotrophic factor (GDNF) that is essential for ureteric bud outgrowth during kidney development (Brophy et al., 2001). Within a specific organ, comparison of the normal expression pattern of a transcription factor with regions that are affected by the loss of this gene product can sometimes reveal non-cell autonomous role(s) of the transcription factor.

Our inner ear analysis of *Pax2* knockout mice indicates that there is a good correlation between *Pax2* expression domains and regions that are affected by the loss of *Pax2* gene function. For example, *Pax2* is not expressed in the three cristae and semicircular canals, and these structures formed normally in the mutants. The change in the sizes of the canals and ampullae are most likely indirect and due to defects in endolymphatic duct/sac function. On the other hand, *Pax2* expression overlaps with the *Lfng* expression domain medially at 10.5 dpc that presumably includes the prospective maculae and the organ of Corti. While the macula utriculi forms normally, the macula sacculi is often affected. In the cochlear anlage, the *Pax2* expression domain is initially very broad, spanning the medial and posterior domains at 10.5 dpc (Fig. 9A, blue color; Figs. 3A, C). If one projects this expression domain of *Pax2* onto a cochlea at 15.5 dpc, it would span from the *Lfng* positive, sensory region to the border of the stria vascularis and the Reissner's membrane, even though *Pax2* transcripts are only detected in the stria vascularis by 15.5 dpc. Interestingly, defects in

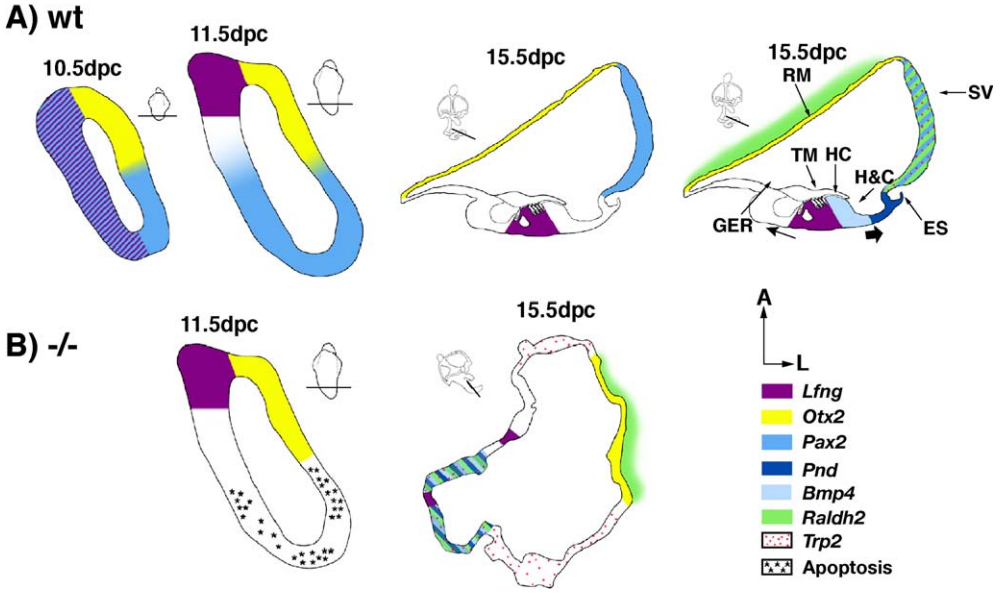

Fig. 9. A schematic diagram summarizing gene expression patterns in wild-type and *Pax2* mutant cochlea. (A) Expression patterns of *Lfng*, *Pax2* and *Otx2* in the developing cochlear region at 10.5, 11.5 and 15.5 dpc. There is a relative shift of these expression domains within the growing cochlea over time. The medial sensory region of the cochlea (purple color) at 10.5 dpc is shifted to the posterior wall of the cochlear duct. The *Otx2* positive region (yellow color) in the antero-lateral domain at 10.5 dpc (Morsli et al., 1999) is shifted to the anterior wall of the cochlear duct, the Reissner's membrane, at 15.5 dpc. The *Pax2* positive region (blue color) at 10.5 dpc is in the medial and posterior regions, and it overlaps with the *Lfng* positive region (blue and purple hatched lines). At 11.5 dpc, the *Pax2* positive region is restricted toward the posterior region of the presumptive cochlea that develops into the lateral wall of the cochlear duct, the stria vascularis, by 15.5 dpc. Also, the *Pax2* positive domain at 10.5 dpc (blue color in A) differentiates into various regions including, sensory (*Lfng* positive, purple color), Hensen's and Claudius' cells (H and C, *Bmp4* positive, light blue color), external sulcus (ES; *Pnd* positive, dark blue color), and stria vascularis by 15.5 dpc (*Pax2*, *Raldh2* and *Trp2* positive that are represented by blue, green and red colors, respectively). (B) In the *Pax2* mutants, massive cell death (black asterisks) occurs at 11.5 dpc in the region that normally expresses *Pax2*. As a result, the relative regional shift within the cochlear duct does not occur, and *Lfng* and *Otx2* expression domains maintain their medial and lateral locations, respectively, similar to a wild-type inner ear at 10.5 dpc (A). In addition, various cochlear regions fail to compartmentalize properly: *Lfng*, *Bmp4*, *Pnd*, *Raldh2*, and *Trp2* are co-localized in the same region. The approximate plane of section for each stage is shown in the corresponding inner ear diagram. An arrow and block arrow in A point toward the neural and abneural sides of the cochlear duct, respectively. Abbreviations: ES, external sulcus; HC, hair cells; H and C, Hensen's and Claudius' cells; GER, greater epithelial ridge; RM, Reissner's membrane; SV, stria vascularis; TM, tectorial membrane. Orientation arrows: A, anterior; L, lateral; applies to all panels.

the cochlea of *Pax2* mutants involve multiple regions, especially from the sensory region to the stria vascularis, corresponding to this projected expression domain of *Pax2* from 10.5 dpc.

Pax2 transcripts are not detected in the cochleo-vestibular ganglion. There is no obvious defect in the delamination of neuroblasts at 10.5 dpc, and no increase in apoptosis up to 11.5 dpc in the *Pax2* mutants. The loss of neurons in both vestibular and spiral ganglia later in development could be due to a lack of normal neurotrophic supply from the sensory tissues, even though improper projection of these neurons to nuclei in the central nervous system could also be involved.

In non-sensory regions, a fusion of the endolymphatic duct and common crus occurs in all *Pax2* mutants examined. The presence of *Pax2* in the endolymphatic duct as well as the lateral region of the common crus could both contribute to the failure of separation between these two structures. The correspondence of the sensory and non-sensory defects in the *Pax2* mutants with the normal expression domains of *Pax2* within the inner ear suggests that *Pax2* primarily plays a cell autonomous role within the inner ear. However, we cannot rule out the possibility that the neural tube defect in *Pax2* mutants also contributes to the inner ear phenotype observed because the inner ears are more severely affected in mutants with exencephaly.

Pax2 and hair cell formation

Pax2 is expressed in all the nascent sensory hair cells in the mouse (Lawoko-Kerali et al., 2002). In the zebrafish inner ear, *pax2.1*, a homolog of *Pax2*, is thought to interact with the Notch signaling pathway in mediating the number of sensory hair cells (Riley et al., 1999). Zebrafish generate hair cells at an early stage of inner ear development, whereas hair cell genesis is a relatively later event in mice. *Pax2* appears to have earlier roles in proper morphogenesis of the mouse inner ear, including the sensory tissue development of the macula sacculi and organ of Corti. We did not determine if lack of *Pax2* increases the number of hair cells in mice as it does in zebrafish. Nevertheless, hair cells do appear to form normally in *Pax2* mutant mice.

Pax2 in cochlear development

The cochlear duct develops from the ventral portion of the otic vesicle. The molecular mechanisms underlying the morphogenesis of the cochlear duct are largely unknown. In the mouse, the anlage of the cochlear duct first extends ventrally in an antero-medial direction and then coils laterally to form 1.75 turns (Morsli et al., 1998). In addition to changes in the orientation of the cochlear duct during its outgrowth, there is also a positional shift of different regions within the cochlear duct, based on expression patterns of three genes, *Lfng*, *Pax2* and *Otx2* (Fig. 9A). At 10.5 dpc, the *Lfng* positive domain (Fig. 9A, purple color) that includes the presumptive sensory tissues of the cochlea spans the medial region of the cochlear anlage, and this *Lfng* domain is more restricted at 11.5 dpc. By 15.5 dpc, the sensory tissue of the cochlea is localized to a small region in the posterior wall of the cochlear duct. At 10.5 dpc, the *Pax2* positive domain (Fig. 9A, blue color) encompasses the medial and posterior regions of the cochlear anlage. *Pax2* expression is quickly restricted to mostly the posterior region of this anlage at 11.5 dpc and is localized to the stria vascularis, the lateral wall of the cochlear duct by 15.5 dpc (Fig. 9A). The *Otx2* domain (Fig. 9A, yellow color; Morsli et al., 1999) which is located in the lateral region of the cochlear anlage, is in the Reissner's membrane, the anterior wall of the cochlear duct, by 15.5 dpc. On the basis of these relative changes in expression domains over time, we extrapolate that there is a relative shift of regions within the cochlear duct during development such that the medial, posterior and lateral walls of a cochlear anlage form the posterior, lateral and anterior walls of a mature cochlear duct, respectively (Fig. 9A).

The lack of *Pax2* causes massive cell death in the presumptive cochlear duct. As a result, morphogenesis is affected. The cochlear duct fails to extend normally based on paint-fill analysis. The positions of the *Lfng* and *Otx2* domains resemble the orientation of a normal cochlear duct at 10.5 or 11.5 dpc rather than at 15.5 dpc (Figs. 9A, B), suggesting that the lack of *Pax2* also affects the relative regional shift within the cochlear duct. The overlap of the *Bmp4* expression domain with that of *Lfng* in mutant cochlea at 15.5 dpc also resembles the wild-type pattern at early stages (Morsli et al., 1998). Together, these results indicate that there is an arrest of cochlear development in *Pax2* mutants starting around 11.5 dpc. It is not clear how the relative shift in domains normally relates to the global extension and coiling of the cochlear duct. An attractive hypothesis is that differential growth within various domains of the cochlear duct, governed by genes such as *Pax2* and *Otx*, is a major force responsible for proper extension, orientation, and coiling of the cochlear duct. In line with this hypothesis, analyses of knockout mice show that both *Otx1* and *Otx2* are important for the proper coiling and growth of the cochlear duct (Cantos et al., 2000; Morsli et al., 1999). However, the cochlear phenotypes resulting from the lack of *Otx1* and *Otx2* are not as rudimentary as those shown here for the *Pax2* −/− inner ears, suggesting that *Pax2* plays an earlier and more important role in proper outgrowth and coiling of the cochlear duct.

Despite the arrest of cochlear outgrowth, some later appearing cochlear genes such as *Pnd*, *Trp2* and *Raldh2* are activated in the mutant cochlear duct, even though their expression domains are aberrant. The *Bmp4*, *Pnd*, *Trp2*, *Raldh2* expression domains, which are in separate compartments spanning from the outer hair cell region to the stria vascularis in a normal cochlea, are all co-localized in the mutants, together with some of the sensory tissues (Fig. 9B). It is not clear if the co-localization of some of these genes in

the same region represents a mixing of cells that have undergone relative normal fate specification but have abnormal positions within the cochlea due to a lack of proper morphogenesis. Alternatively, it is possible that cells between the sensory region and the stria vascularis share a common lineage within a normal cochlear anlage. If so, the lack of *Pax2* may affect the proper cell fate specification in this region and cause aberrant co-expression of genes that are normally expressed in separate cell types and regions of the cochlea. Interestingly, cell lineage studies using replication defective retroviruses have demonstrated a common lineage between supporting cells and cells in the abneural region of the cochlear duct in chicken (Fekete et al., 1998). Therefore, it is conceivable that the mutant phenotype is primarily due to a failure of cell fate specification. There is additional evidence that suggests cell fate specification is not normal in the mutant inner ear. The aberrant locations of the neural crest derived, *Trp2* positive melanocytes in the mutants suggests that cell signaling in the cochlea that normally attracts the melanocytes to the correct region of the cochlear duct is disrupted.

In contrast, the region outside of the *Pax2* expression domain, the Reissner's membrane, appears relatively normal in the mutants, based on the expression of *Otx2* in the epithelium and *Raldh2* in the adjacent mesenchyme (Fig. 9B). These results further support the hypothesis of a cell autonomous role of *Pax2* in cochlear development.

Upstream regulators and downstream targets of Pax2 in inner ear development

In *Drosophila* eye imaginal disc, the *pax6* gene, *ey*, functions upstream of both *eya* and *so* (*sine oculis*, a *Six* homolog; Halder et al., 1998). Expression of both *Eya1* and *Eya2* are also dependent on Pax6 activity during mammalian eye development (Xu et al., 1997). However, while a eya-six relationship may occur in the inner ear (Xu et al., 1999; Zheng et al., 2003), it is not clear if *Pax2* acts upstream of *Eya1* and *Six1* in this organ. First, neither *Eya1* nor *Six1* expression is affected in *Pax2* mutants (Xu et al., 2003; Fig. 6F). Second, both *Eya1* and *Six1* knockout mice display much more severe inner ear defects than *Pax2* mutants (Ozaki et al., 2004; Xu et al., 1999, 2003). These results suggest that *Eya1* and *Six1* are not direct downstream targets of *Pax2*. However, it is conceivable that *Pax2* shares redundant functions with other *Pax* genes in the inner ear and that these *Pax* genes maintain *Eya1* and *Six1* expression in *Pax2* mutants. *Pax8*, another member of the *Pax 2-5-8* subclass of *Pax* genes shares homology with *Pax2* and has an expression domain similar to that of *Pax2* in the otocyst (Xu et al., 1999, 2003). *Pax8*, however, does not seem to be required for the proper morphogenesis of the inner ear. Our preliminary paint-fill analysis of perinatal *Pax8* −/− inner ears indicates that their gross anatomy is normal (Schwarz and Wu, unpublished observation). A delay in tissue maturation of the *Pax8* −/− inner ears due to the lack of thyroid gland in these animals has also been reported (Christ et al., 2004). The inner ears of a double knock out of *Pax2* and *Pax8* remain to be evaluated. Nevertheless, based on the overlapping but different expression patterns of the two *Pax* genes with *Eya1* and *Six1* in the developing mouse inner ear, a pax-eya-six hierarchy, if it exists, would most likely be region-specific, rather than present in all otic epithelial cells (Kalatzis et al., 1998; Ozaki et al., 2004; Xu et al., 2003).

A complementary relationship of Pax2 and Gata3 expression patterns exists in the dorsal region of the mouse otocyst (Lawoko-Kerali et al., 2002). The lack of *Pax2* could result in an expansion of *Gata3* expression domain. However, such expansion was not observed in the *Pax2* −/− otocysts (data not shown). In the cochlea where the expression patterns of both genes overlap, the expression of *Gata3* is usually reduced. In addition to *Gata3*, the expression patterns of other genes such as *Pnd*, *Bmp4* and *Raldh2* are also aberrant in the *Pax2* −/− cochlear ducts. However, because these genes are all activated in the *Pax2* mutant inner ears indicate that the expression of these genes does not require *Pax2*. Direct downstream targets of Pax2 remain elusive. Our BrdU and apoptosis studies indicate that *Pax2* is normally expressed in a region that undergoes active proliferation in the cochlea (compare Fig. 5H with Figs. 3G and I), and the lack of Pax2 activity affects the survival of cells within the *Pax2* expression domain (Fig. 5I). Taken together, we postulate that downstream targets of Pax2 are most likely involved in cell proliferation and survival, in a cell autonomous fashion.

Pax2 is one of the earliest genes to be activated in the otic placode (Nornes et al., 1990; Puschel et al., 1992; Rinkwitz-Brandt et al., 1995, 1996). It is not clear what factors induce *Pax2* expression in the otic placode. The maintenance of *Pax2* expression in the inner ear is thought to require Sonic hedgehog (Riccomagno et al., 2002).

Pax2 mutants as animal models for human deafness syndromes

Pax2 knock out mice were reported to display agenesis of the cochlea and the absence of the spiral ganglion (Torres et al., 1996). Our analyses indicate that the cochlear phenotype is less severe than reported. However, this difference in severity of cochlear phenotype could be due to a difference in the genetic background. The earlier study was conducted with mice on a 129sv background, while this study was conducted primarily with mice with a mixed 129sv/C57BL/6 background. It is possible that the phenotype is more severe in a pure 129sv background. When we backcross the *Pax2* line with a mixed 129S6/C57BL/6 hybrid line (Taconic) instead of C57BL/6, we detect a small percentage of heterozygous mice with an abnormal inner ear phenotype (based on paint-fill analysis, one out of nine heterozygotes from three litters), even though the homozygous phenotype ($n = 3$) is similar to the ones generated by crossing with C57BL/6 mice. Variable penetrance of exen-

cephaly in *Pax2* heterozygotes due to differences in genetic background has been observed (Torres et al., 1996).

Nevertheless, the inner ear phenotype described here closely resembles the inner ears of *Pax2*^{1neu} mice which carry a mutation in *Pax2* that is identical to a human family segregating renal-coloboma syndrome (Favor et al., 1996). The inner ears of *Pax2*^{1neu} mice were described as missing a saccule and to have an enlarged ventral portion continuous with the enlarged endolymphatic duct. Gross abnormalities were similar to the mutant, paint-filled ears shown here. The similarities in inner ear phenotypes between the knockout and *Pax2*^{1neu} suggest that the frameshift mutation most likely resulted in a functionally null Pax2 protein, as previously proposed (Favor et al., 1996).

Interestingly, some patients with renal-coloboma syndromes suffer from high frequency hearing loss (Sanyanusin et al., 1995; Schimmenti et al., 1997). Even though the etiology of the hearing loss is not known in these patients and the gross anatomy of the inner ears has not been examined, their defects could be a very mild form of the phenotypes observed in mice. Despite the repertoire of genes analyzed in the *Pax2* mutants, immediate downstream targets of *Pax2* remain elusive. A global comparison of gene expression between wild-type and mutant otocysts using microarray approaches may provide candidates for direct downstream targets of *Pax2*. Therefore, these mutant lines will continue to serve as important tools in deciphering the etiology of syndromes associated with human deafness.

Acknowledgments

We thank Drs. Martin Schwarz and Peter Gruss for *Pax8* knockout embryos, Dr. Bernd Fritzsch for advice on ganglion identification, Dr. Zhengshi Lin in our laboratory for performing anti-BrdU staining, and Drs. Susan Sullivan and Thomas Friedman for critical reading of the manuscript. We also thank Drs. Ursula Drager, Tom Friedman, Eric Green, Peter Gruss, Alar Karis, Qiufu Ma, Richard Maas, Antonio Simeone, and Karen Steel for plasmids.

References

Abdelhak, S., Kalatzis, V., Heilig, R., Compain, S., Samson, D., Vincent, C., Weil, D., Cruaud, C., Sahly, I., Leibovici, M., Bitner-Glindzicz, M., Francis, M., Lacombe, D., Vigneron, J., Charachon, R., Boven, K., Bedbeder, P., Van Regemorter, N., Weissenbach, J., Petit, C., 1997. A human homologue of the *Drosophila* eyes absent gene underlies branchio-oto-renal (BOR) syndrome and identifies a novel gene family. Nat. Genet. 15, 157–164.

Anderson, D.W., Probst, F.J., Belyantseva, I.A., Fridell, R.A., Beyer, L., Martin, D.M., Wu, D., Kachar, B., Friedman, T.B., Raphael, Y., Camper, S.A., 2000. The motor and tail regions of myosin XV are critical for normal structure and function of auditory and vestibular hair cells. Hum. Mol. Genet. 9, 1729–1738.

Brophy, P.D., Ostrom, L., Lang, K.M., Dressler, G.R., 2001. Regulation of ureteric bud outgrowth by Pax2-dependent activation of the glial derived neurotrophic factor gene. Development 128, 4747–4756.

Cantos, R., Cole, L.K., Acampora, D., Simeone, A., Wu, D.K., 2000. Patterning of the mammalian cochlea. Proc. Natl. Acad. Sci. U. S. A. 97, 11707–11713.

Christ, S., Biebel, U.W., Hoidis, S., Friedrichsen, S., Bauer, K., Smolders, J.W., 2004. Hearing loss in athyroid pax8 knockout mice and effects of thyroxine substitution. Audiol. Neuro-otol. 9, 88–106.

Dressler, G.R., Deutsch, U., Chowdhury, K., Nornes, H.O., Gruss, P., 1990. Pax2, a new murine paired-box-containing gene and its expression in the developing excretory system. Development 109, 787–795.

Everett, L.A., Morsli, H., Wu, D.K., Green, E.D., 1999. Expression pattern of the mouse ortholog of the Pendred's syndrome gene (Pds) suggests a key role for pendrin in the inner ear. Proc. Natl. Acad. Sci. U. S. A. 96, 9727–9732.

Everett, L.A., Belyantseva, I.A., Noben-Trauth, K., Cantos, R., Chen, A., Thakkar, S., Hoogstraten-Miller, S., Kachar, B., Wu, D.K., Green, E., 2001. Targeted disruption of mouse Pds provides key insight about the inner-ear defects encountered in Pendred syndrome. Hum. Mol. Genet. 10, 153–161.

Favor, J., Sandulache, R., Neuhauser-Klaus, A., Pretsch, W., Chatterjee, B., Senft, E., Wurst, W., Blanquet, V., Grimes, P., Sporle, R., Schughart, K., 1996. The mouse Pax2(1Neu) mutation is identical to a human PAX2 mutation in a family with renal-coloboma syndrome and results in developmental defects of the brain, ear, eye, and kidney. Proc. Natl. Acad. Sci. U. S. A. 93, 13870–13875.

Fekete, D.M., Muthukumar, S., Karagogeos, D., 1998. Hair cells and supporting cells share a common progenitor in the avian inner ear. J. Neurosci. 18, 7811–7821.

Halder, G., Callaerts, P., Flister, S., Walldorf, U., Kloter, U., Gehring, W.J., 1998. Eyeless initiates the expression of both sine oculis and eyes absent during *Drosophila* compound eye development. Development 125, 2181–2191.

Hulander, M., Kiernan, A.E., Blomqvist, S.R., Carlsson, P., Samuelsson, E.J., Johansson, B.R., Steel, K.P., Enerback, S., 2003. Lack of pendrin expression leads to deafness and expansion of the endolymphatic compartment in inner ears of Foxi1 null mutant mice. Development 130, 2013–2025.

Kalatzis, V., Sahly, I., El-Amraoui, A., Petit, C., 1998. Eya1 expression in the developing ear and kidney: towards the understanding of the pathogenesis of Branchio-Oto-Renal (BOR) syndrome. Dev. Dyn. 213, 486–499.

Karis, A., Pata, I., van Doorninck, J.H., Grosveld, F., de Zeeuw, C.I., de Caprona, D., Fritzsch, B., 2001. Transcription factor GATA-3 alters pathway selection of olivocochlear neurons and affects morphogenesis of the ear. J. Comp. Neurol. 429, 615–630.

Keller, S.A., Jones, J.M., Boyle, A., Barrow, L.L., Killen, P.D., Green, D.G., Kapousta, N.V., Hitchcock, P.F., Swank, R.T., Meisler, M.H., 1994. Kidney and retinal defects (Krd), a transgene-induced mutation with a deletion of mouse chromosome 19 that includes the Pax2 locus. Genomics 23, 309–320.

Kim, W.Y., Fritzsch, B., Serls, A., Bakel, L.A., Huang, E.J., Reichardt, L.F., Barth, D.S., Lee, J.E., 2001. NeuroD-null mice are deaf due to a severe loss of the inner ear sensory neurons during development. Development 128, 417–426.

Lawoko-Kerali, G., Rivolta, M.N., Holley, M., 2002. Expression of the transcription factors GATA3 and Pax2 during development of the mammalian inner ear. J. Comp. Neurol. 442, 378–391.

Liu, M., Pereira, F.A., Price, S.D., Chu, M., Shope, C., Himes, D., Eatock, R.A., Brownell, W.E., Lysakowski, A., Tsai, M.J., 2000. Essential role of BETA2/NeuroD1 in development of the vestibular and auditory systems. Genes Dev. 14, 2839–2854.

Ma, Q., Chen, Z., Barrantes, I., de la Pompa, J.L., Anderson, D.J., 1998. Neurogenin 1 is essential for the determination of neuronal precursors for proximal cranial sensory ganglia. Neuron 20, 469–482.

Morrison, A., Hodgetts, C., Gossler, A., Hrabe de Angelis, M., Lewis, J.,

1999. Expression of Delta1 and Serrate1 (Jagged1) in the mouse inner ear. Mech. Dev. 84, 169–172.

Morsli, H., Choo, D., Ryan, A., Johnson, R., Wu, D.K., 1998. Development of the mouse inner ear and origin of its sensory organs. J. Neurosci. 18, 3327–3335.

Morsli, H., Tuorto, F., Choo, D., Postiglione, M.P., Simeone, A., Wu, D.K., 1999. Otx1 and Otx2 activities are required for the normal development of the mouse inner ear. Development 126, 2335–2343.

Nornes, H.O., Dressler, G.R., Knapik, E.W., Deutsch, U., Gruss, P., 1990. Spatially and temporally restricted expression of Pax2 during murine neurogenesis. Development 109, 797–809.

Ozaki, H., Nakamura, K., Funahashi, J., Ikeda, K., Yamada, G., Tokano, H., Okamura, H.O., Kitamura, K., Muto, S., Kotaki, H., Sudo, K., Horai, R., Iwakura, Y., Kawakami, K., 2004. Six1 controls patterning of the mouse otic vesicle. Development 131, 551–562.

Puschel, A.W., Westerfield, M., Dressler, G.R., 1992. Comparative analysis of Pax-2 protein distributions during neurulation in mice and zebrafish. Mech. Dev. 38, 197–208.

Riccomagno, M.M., Martinu, L., Mulheisen, M., Wu, D.K., Epstein, D.J., 2002. Specification of the mammalian cochlea is dependent on Sonic hedgehog. Genes Dev. 16, 2365–2378.

Riley, B.B., Chiang, M., Farmer, L., Heck, R., 1999. The deltaA gene of zebrafish mediates lateral inhibition of hair cells in the inner ear and is regulated by pax2.1. Development 126, 5669–5678.

Rinkwitz-Brandt, S., Justus, M., Oldenettel, I., Arnold, H.H., Bober, E., 1995. Distinct temporal expression of mouse Nkx-5.1 and Nkx-5.2 homeobox genes during brain and ear development. Mech. Dev. 52, 371–381.

Rinkwitz-Brandt, S., Arnold, H.H., Bober, E., 1996. Regionalized expression of Nkx5-1, Nkx5-2, Pax2 and sek genes during mouse inner ear development. Hear. Res. 99, 129–138.

Romand, R., Albuisson, E., Niederreither, K., Fraulob, V., Chambon, P., Dolle, P., 2001. Specific expression of the retinoic acid-synthesizing enzyme RALDH2 during mouse inner ear development. Mech. Dev. 106, 185–189.

Royaux, I.E., Belyantseva, I.A., Wu, T., Kachar, B., Everett, L.A., Marcus, D.C., Green, E.D., 2003. Localization and functional studies of pendrinin the mouse inner ear provide insight about the etiology of deafness in pendred syndrome. J. Assoc. Res. Otolaryngol. 4, 394–404.

Sanyanusin, P., Schimmenti, L.A., McNoe, L.A., Ward, T.A., Pierpont, M.E., Sullivan, M.J., Dobyns, W.B., Eccles, M.R., 1995. Mutation of the PAX2 gene in a family with optic nerve colobomas, renal anomalies and vesicoureteral reflux. Nat. Genet. 9, 358–364.

Schimmenti, L.A., Cunliffe, H.E., McNoe, L.A., Ward, T.A., French, M.C., Shim, H.H., Zhang, Y.H., Proesmans, W., Leys, A., Byerly, K.A., Braddock, S.R., Masuno, M., Imaizumi, K., Devriendt, K., Eccles, M.R., 1997. Further delineation of renal-coloboma syndrome in patients with extreme variability of phenotype and identical PAX2 mutations. Am. J. Hum. Genet. 60, 869–878.

Steel, K.P., Davidson, D.R., Jackson, I.J., 1992. TRP-2/DT, a new early melanoblast marker, shows that steel growth factor (c-kit ligand) is a survival factor. Development 115, 1111–1119.

Torres, M., Gomez-Pardo, E., Dressler, G.R., Gruss, P., 1995. Pax-2 controls multiple steps of urogenital development. Development 121, 4057–4065.

Torres, M., Gomez-Pardo, E., Gruss, P., 1996. Pax2 contributes to inner ear patterning and optic nerve trajectory. Development 122, 3381–3391.

Van Esch, H., Groenen, P., Nesbit, M.A., Schuffenhauer, S., Lichtner, P., Vanderlinden, G., Harding, B., Beetz, R., Bilous, R.W., Holdaway, I., Shaw, N.J., Fryns, J.P., Van de Ven, W., Thakker, R.V., Devriendt, K., 2000. GATA3 haplo-insufficiency causes human HDR syndrome. Nature 406, 419–422.

Xu, P.X., Woo, I., Her, H., Beier, D.R., Maas, R.L., 1997. Mouse Eya homologues of the *Drosophila* eyes absent gene require Pax6 for expression in lens and nasal placode. Development 124, 219–231.

Xu, P.X., Adams, J., Peters, H., Brown, M.C., Heaney, S., Maas, R., 1999. Eya1-deficient mice lack ears and kidneys and show abnormal apoptosis of organ primordia. Nat. Genet. 23, 113–117.

Xu, P.X., Zheng, W., Huang, L., Maire, P., Laclef, C., Silvius, D., 2003. Six1 is required for the early organogenesis of mammalian kidney. Development 130, 3085–3094.

Zhao, D., McCaffery, P., Ivins, K.J., Neve, R.L., Hogan, P., Chin, W.W., Drager, U.C., 1996. Molecular identification of a major retinoic-acid-synthesizing enzyme, a retinaldehyde-specific dehydrogenase. Eur. J. Biochem. 240, 15–22.

Zheng, W., Huang, L., Wei, Z.B., Silvius, D., Tang, B., Xu, P.X., 2003. The role of Six1 in mammalian auditory system development. Development 130, 3989–4000.